The influence of dopant concentration on the oxygen K-edge ELNES and XANES in yttria-stabilized zirconia



2001 J. Phys.: Condens. Matter 13 10799

(http://iopscience.iop.org/0953-8984/13/48/306)

INSTITUTE OF PHYSICS PUBLISHING JOURNAL OF PHYSICS: CONDENSED MATTER

J. Phys.: Condens. Matter **13** (2001) 10799–10809 PII: S0953-8984(01)28380-5

# The influence of dopant concentration on the oxygen K-edge ELNES and XANES in yttria-stabilized zirconia

**D Vlachos**[1,2,3], **A J Craven**[1] **and D W McComb**[1,4]

[1] Department of Physics and Astronomy, University of Glasgow, Glasgow G12 8QQ, UK
[2] Department of Chemistry, University of Glasgow, Glasgow G12 8QQ, UK

E-mail: D.McComb@chem.gla.ac.uk

Received 22 August 2001, in final form 4 October 2001
Published 16 November 2001
Online at stacks.iop.org/JPhysCM/13/10799

**Abstract**

The electron energy-loss near-edge structure (ELNES) and x-ray absorption near-edge structure (XANES) at the oxygen K-edge has been investigated in a range of yttria-stabilized zirconia (YSZ) materials. The positions of the peaks in the near-edge structure are identical in both techniques. Differences observed in the intensities of the features are attributed to the effect of specimen charging in the XANES experiments. Analysis of near-edge structure reveals that both the crystallographic phase and the metal fraction of yttrium present can be determined directly from the oxygen K-edge data opening up opportunities for characterization of interfacial phenomena in YSZ materials with sub-nanometre resolution using ELNES.

## 1. Introduction

Yttria-stabilized zirconia (YSZ) has been the subject of many experimental and theoretical studies due to the commercial applications of zirconia-based materials [1, 2]. YSZ is formed by the addition of $Y_2O_3$ to $ZrO_2$ and results in the stabilisation of the tetragonal or cubic phase depending on the molar fraction of $Y_2O_3$. While $Y_2O_3$ is probably the most widely used, stabilisation using other binary oxides such as CaO, MgO and $La_2O_3$ is also possible. Pure $ZrO_2$ exhibits three well defined polymorphs at ambient pressure: monoclinic ($<$1170 °C), tetragonal (1170–2370 °C) and cubic (2370–2680 °C) [3]. In addition, it has been reported that monoclinic $ZrO_2$ can be transformed into orthorhombic and hexagonal phases under high pressure [4]. The $Zr^{4+}$ ion in monoclinic $ZrO_2$ is found in sevenfold coordination with the oxygen anions, while in the tetragonal phase the Zr cation is located in a distorted eightfold coordination environment. On average the high-temperature cubic phase has the fluorite ($CaF_2$)

[3] Now at Department of Physics, University of Ioannina, Greece.
[4] Author to whom correspondence should be addressed.

0953-8984/01/4810799+11$30.00  

structure with each metal ion in regular eightfold coordination sites with all of the Zr–O bonds of equal length. However, there is clear evidence of large vibration amplitudes about the average oxygen position [5, 6]. Yttria has a large solid solubility range in $ZrO_2$ and hence can be used to stabilise both the tetragonal and cubic phases.

In YSZ the aliovalent dopant cations, $Y^{3+}$ substitute for some of the $Zr^{4+}$ ions and in order to maintain charge neutrality, assuming formal ionic charges, one oxygen vacancy must be created for each pair of dopant cations. The presence of anion vacancies in YSZ reduces the average cation coordination number from 8, as in pure tetragonal or cubic $ZrO_2$, to a value between 7 and 8 depending on the dopant concentration. Though the exact nature of the atomic displacements in YSZ remains unclear, one can suppose that the relaxation of the ions away from their regular lattice sites results in local coordination environments more similar to those found in m-$ZrO_2$ [5–7]. Recent x-ray and neutron diffraction experiments suggest that the cubic YSZ phase contains 'locally ordered regions of vacancies and dopants' [8]. It has been reported that at low concentrations of $Y_2O_3$ there are small regions (15–20 Å) that contain isolated anion vacancies as well as vacancy pairs arranged on the nearest-neighbour anion sites in the $\langle 111 \rangle$ directions, with the cation site located between them occupied by a $Zr^{4+}$ ion [8]. Goff and co-workers [8] suggested that another type of defect cluster formed as the $Y_2O_3$ content increases: the $\langle 111 \rangle$ vacancy pairs pack together to form aggregates whose size and number increase slightly with $Y_2O_3$ concentration. The number of the isolated vacancies also increases with yttria content. It is thought that these isolated vacancies become mobile above 1000 K, resulting in a rise of the ionic conductivity of YSZ [9]. Further investigation of the complex YSZ crystal structure to improve understanding of the local coordination and bonding environments is necessary. Despite numerous investigations, no full quantitative description of the stabilisation mechanism of YSZ has been reported. Extended x-ray absorption fine structure (EXAFS) can distinguish between the host and dopant cations, allowing the individual coordination polyhedra to be probed [10]. However, EXAFS studies published to date are somewhat contradictory: several studies have concluded that an Y ion is nearest neighbour to the vacancy while others have reported that yttrium occupies next-nearest neighbour cation sites [10, 11]. These inconsistencies are partly due to experiments being performed on samples with different dopant concentrations leading to different displacements of the regular fluorite lattice sites near to the vacancies.

Electron-energy-loss spectroscopy (EELS) via analysis of the energy-loss near-edge structure (ELNES) has developed into a powerful technique for the investigation of the unoccupied electronic states of crystals [12]. This is especially true when the technique is carried out in a modern analytical electron microscope as this enables information to be obtained with high spatial resolution. ELNES results when the energetic incoming electron excites a core level electron into an empty state above the Fermi level. Analysis of the energy lost by the fast electron results in an electron energy-loss spectrum that contains ionisation edges at the energies associated with the elements present in the material. ELNES can be considered as the electron analogue of the more established x-ray absorption near-edge structure (XANES) technique. In XANES the incident x-ray photon radiation can eject a bound atomic electron, giving rise to an absorption edge. It has been recognized for many years that the fine structure up to about 50 eV beyond the onset of this edge provides important information about the electronic, structural and chemical properties of the material [13]. In principle, the same electronic transitions are probed by both techniques and, to a first approximation, the intensity in both is controlled by the dipole transition matrix element between the initial and final states. Thus the information obtained is localized to the site of the excitation by the localized nature of the initial state and gives information on the unoccupied density of states (DOS) on that site with symmetries allowed by the dipole selection rule $\Delta\ell = \pm 1$. This means that an electron

occupying an s orbital in the initial state will be excited into an unoccupied p like state, while one in a p orbital will be excited into an empty s or d like state. Hence, XANES and ELNES are probes of the site and symmetry-projected density of unoccupied electronic states around the excited atom. Considering the theoretical correlation [14] between the techniques it is somewhat remarkable that few experimental studies that compare in detail the results of the two methods have been published.

Since ELNES and XANES data are related to the unoccupied DOS, it is possible to compare the spectra directly with the results of density functional theory (DFT) calculations. This approach has been used in the past by many authors utilizing a number of different reciprocal-space and real-space band structure methods [15]. However, the calculation is complicated by the core hole produced during the excitation process. This influences the ELNES/XANES spectrum by distorting the local DOS in the vicinity of the excited atom and means that the correspondence between the calculated angular-momentum-projected DOS and experimental intensity is not exact. There are a few models that attempt to take this core hole effect into account. The most widely used is the $Z + 1$ approximation, where the core hole is simulated as an increase in the effective nuclear charge at the excited site [16]. Another model, used recently by Lie and co-workers [17], proposes omission of one of the core shell electrons and the corresponding addition of one electron to the valence band. It has been shown recently that use of Slater's transition-state approximation results in improved agreement between the theoretical and experimental EELS threshold energy [7, 18]. Within this model half of a core hole is retained in order to account for the screening effects that are absent in the one electron approximation.

In the present paper the results of an investigation of the oxygen K edge in a range of YSZ materials are reported. This is part of study whose principle objective is to correlate changes in the near-edge structure with the chemistry and crystallography of the YSZ materials. It is emphasized that in this work the same edge in exactly the same materials has been investigated using both ELNES and XANES. Thus, it is possible to investigate directly the correlation between the techniques.

## 2. Materials and methods

### *2.1. Samples*

The YSZ specimens were synthesized and supplied by MEL Chemicals. Pure zirconia was purchased from Alfa Aesar (Puratronic, 99.978%). The specimens investigated are listed in table 1. The specimens were initially characterized by powder x-ray diffraction (XRD—Philips PW1050/35) to check phase purity. The particle size and chemical homogeneity of the specimens was investigated using a transmission electron microscope (Akashi 002B) fitted with a windowless energy-dispersive x-ray (EDX) analyser (Link QX2000). Specimens were prepared for electron microscopy by breaking up any aggregates in a mortar and pestle followed by dispersion in propanol. A droplet of the dispersion was then placed on a holey-carbon coated copper grid.

### *2.2. ELNES experimental procedure*

The ELNES investigations were carried out using a 100 kV dedicated scanning transmission electron microscope (STEM—VG HB5) fitted with post-specimen lenses and equipped with a parallel electron energy-loss spectrometer (PEELS—GATAN 666) and an EDX analyser (Link eXL). A convergence semi-angle of 11 mrad was used, giving a probe diameter of 1 nm and

**Table 1.** The specimens investigated in this study are listed together with information obtained from powder XRD and TEM analysis.

| | XRD phase detected | Average grain size (nm) | Nominal Y/(Zr+Y) | Average Y/(Zr+Y) | Standard deviation |
|---|---|---|---|---|---|
| $ZrO_2$ | Monoclinic | 113 | — | — | — |
| 3 mol% YSZ | Tetragonal[a] | 76 | 0.058 | 0.055 | 0.021 |
| 5 mol% YSZ | Tetragonal[b] | 169 | 0.095 | 0.072 | 0.032 |
| 10 mol% YSZ | Cubic | 154 | 0.182 | 0.180 | 0.069 |
| 15 mol% YSZ | Cubic | 89 | 0.261 | 0.230 | 0.059 |
| 20 mol% YSZ | Cubic | 38 | 0.333 | 0.255 | 0.108 |
| 25 mol% YSZ | Cubic | 46 | 0.400 | 0.329 | 0.118 |
| 30 mol% YSZ | Cubic | 66 | 0.462 | 0.438 | 0.029[c] |

[a] Estimated 5–10% of monoclinic.
[b] Trace quantity of cubic.
[c] One grain of pure $Y_2O_3$ detected.

a probe current of approximately 0.2 nA. The collection semi-angle used was 12.5 mrad. The spectrometer dispersion energy was calibrated as 0.1 eV per channel and the energy resolution at the zero loss peak (FWHM) was 0.6 eV. A background of the form $AE^{-r}$ was removed from the oxygen K-edge spectra, the low-loss spectrum was used to deconvolute the plural scattering and the spectra were then sharpened by deconvoluting the detector point spread function. The spectra from a number of grains of material were checked for consistency and then summed. Hence the data are averaged over a range of orientations. An EDX spectrum was recorded from each area analysed by PEELS and was used to determine the local yttrium metal fraction (Y/(Y + Zr)).

### *2.3. XANES experimental procedure*

The XANES investigations were carried out using the synchrotron radiation source at Daresbury Laboratory. All of the measurements were performed using the soft x-ray beamline (station 1.1). The powder specimens were intimately mixed with graphite powder (Carbone of America) and pressed into a pellet using a 13 mm die. Some variation was observed in the amount of graphite (40–60 wt%) required in order to ensure the samples were sufficiently conducting for the measurements. The pellets were mounted on tantalum plates using conductive tape and immediately prior to insertion in the vacuum chamber the specimens were gently abraded on using fine filter paper to minimize any signal due to oxygen adsorbed in the graphite on the surface of the pellet [19]. The carbon and oxygen K-edge spectra were recorded using total electron yield (TEY) mode in the energy range 200–630 eV. A nickel-coated spherical grating (1800 lines $mm^{-1}$) was used to record the electron yield signal $I_e$. The incident beam current $I_0$, was recorded using a fine gold mesh placed in the optical path before the specimen.

Despite the presence of graphite, charging of the insulating zirconia grains during spectrum acquisition was a major problem in these experiments. When the incident beam of x-rays irradiates a material, the excited atoms produce secondary and Auger electrons. Consequently, the material becomes electropositive and hence the TEY as measured by the specimen drain current is altered if the material is an electrical insulator. This problem was present in all specimens but was most severe in monoclinic zirconia and in specimens with a high yttria content. The most serious implication of this effect is modification of the relative intensities of the peaks observed in the XANES data compared with those observed in the ELNES data of the same specimen (figure 1). This effect can be corrected using the algorithm described by Vlachos

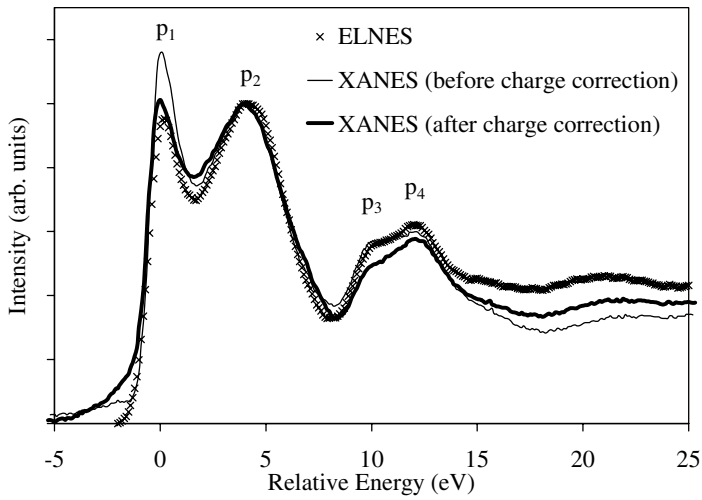


**Figure 1.** Comparison of oxygen K-edge XANES from 10 mol% YSZ before and after charge correction. The ELNES data from the same specimen are also shown. The first peak in each spectrum has been aligned, normalized and set to 0 eV.

*et al* [19]. Figure 1 shows the oxygen K-edge XANES from the 10 mol% YSZ specimen before and after charge correction along with the ELNES data from the same specimen for comparison. In figure 1 the ELNES and XANES spectra have been aligned by setting the energy of the first peak, $p_1$, to 0 eV and have been normalized to the intensity of the second peak, $p_2$. It is clear that after charge correction there is much improved agreement between the relative intensities of the first two peaks, $p_1$ and $p_2$, and the shape of peaks $p_3$ and $p_4$.

## 3. Results and discussion

The samples exhibited the crystallography expected based on their nominal composition (table 1). The powder XRD patterns revealed that while the majority of the materials were phase pure some exhibited the presence of other phases. In particular the 5 mol% YSZ sample contained trace quantities of a cubic YSZ phase while the 3 mol% specimen contained approximately 5–10% monoclinic zirconia. The amount of the m-$ZrO_2$ phase present was estimated measuring the XRD patterns of quantitative mixtures of 3 mol% YSZ and m-$ZrO_2$. The particle size of the powders, measured by TEM, was relatively homogeneous within a given sample but varied non-systematically between specimens. EDX analysis of a large number of grains in each sample was carried out to investigate the distribution of $Y_2O_3$ both within and between grains in each specimen. To measure the homogeneity within each particle a number of EDX spectra were recorded at different points in the grain between the centre and the edge. This type of measurement was performed for each specimen investigated. In table 2 the results of one of these analyses for the 20 mol% YSZ specimen are shown. It is clear that the distribution of $Y_2O_3$ is relatively uniform within the grain and this was found to be the case in all of the specimens investigated.

A comparison of the EDX spectra between a number of grains in each sample provided important information on the overall homogeneity of the $Y_2O_3$ distribution. In the majority of the specimens investigated the $Y_2O_3$ distribution was found to be relatively homogeneous. The results obtained show that the measured yttrium metal fraction is within one standard deviation

**Table 2.** Example of the results obtained from EDX analysis of a number of points on a single grain of 20 mol% YSZ powder. The measured peak areas were corrected for the x-ray cross-section to obtain the ratio of Y/(Y+Zr).

| Point | Y/(Y+Zr) | Error |
|---|---|---|
| 1 | 0.39 | 0.05 |
| 2 | 0.36 | 0.05 |
| 3 | 0.38 | 0.05 |
| 4 | 0.40 | 0.05 |
| 5 | 0.38 | 0.06 |
| 6 | 0.34 | 0.05 |
| 7 | 0.36 | 0.05 |
| 8 | 0.36 | 0.08 |
| 9 | 0.38 | 0.04 |
| 10 | 0.40 | 0.05 |
| 11 | 0.38 | 0.03 |

of the nominal value and for the majority of specimens is very close to the target composition (table 1). However, in the 20 and 25 mol% YSZ samples the $Y_2O_3$ distribution was found to be very inhomogeneous as evidenced by the large standard deviations of the average yttrium metal fraction measured in both materials. This observation does not present any difficulties in the ELNES investigations as the local yttrium metal fraction can be measured using EDX spectroscopy in each grain analysed. In the case of the XANES studies it is necessary to bear in mind that the signal is averaged over a large number of grains and in the two specimens highlighted these grains are not necessarily of the same composition.

Figure 2(*a*) shows the oxygen K-ELNES data from the range of zirconia samples investigated. The spectra displayed were recorded from particles that exhibited an yttrium metal fraction (Y/(Y + Zr)) that is close to the nominal value as measured by EDX. To ensure clarity in the discussion of the changes in ELNES that occur as the $Y_2O_3$ concentration varies it is helpful to subdivide the spectra into three energy regions: energy region 1 (ER1) is defined from the edge threshold to 8 eV, energy region 2 (ER2) from 8 to 14 eV and energy region 3 (ER3) from 14 to 25 eV. These regions are indicated by the dashed vertical lines in figure 2.

ER1 contains two peaks, $p_1$ and $p_2$ in all of the specimens examined. The depth of the minimum between these peaks changes as the $Y_2O_3$ concentration varies. Specifically, the 3 and 5 mol% YSZ samples exhibit a more pronounced minimum than either pure m-$ZrO_2$ or the 10, 20 and 30 mol% YSZ samples. As shown in table 1 these samples differ in crystallography and it appears that a pronounced minimum between $p_1$ and $p_2$ is a characteristic feature of the tetragonal phase. Perhaps the most significant observation in ER1 is that there appears to be an increase in the energy difference between $p_1$ and $p_2$ as the $Y_2O_3$ concentration increases. This observation will be discussed in more detail later. The depth and width of the minimum between ER1 and ER2 also varies with sample composition. In particular this minimum is relatively shallow and broad in the case of m-$ZrO_2$, becomes deeper in the tetragonal specimens then finally narrows in the cubic samples.

In ER2 a rather broad feature is observed that consists of two peaks, $p_3$ and $p_4$. In the monoclinic phase the two peaks are relatively weak and the splitting between them is not very clear. In contrast, in tetragonal materials (3 and 5 mol% YSZ) the two peaks are easily resolvable, appear to be similar in intensity and the splitting between them is quite distinct. Finally in the cubic phases (10, 20 and 30 mol% YSZ) it appears that $p_4$ is significantly more intense than $p_3$ and the splitting between them is less distinct than in the tetragonal materials.

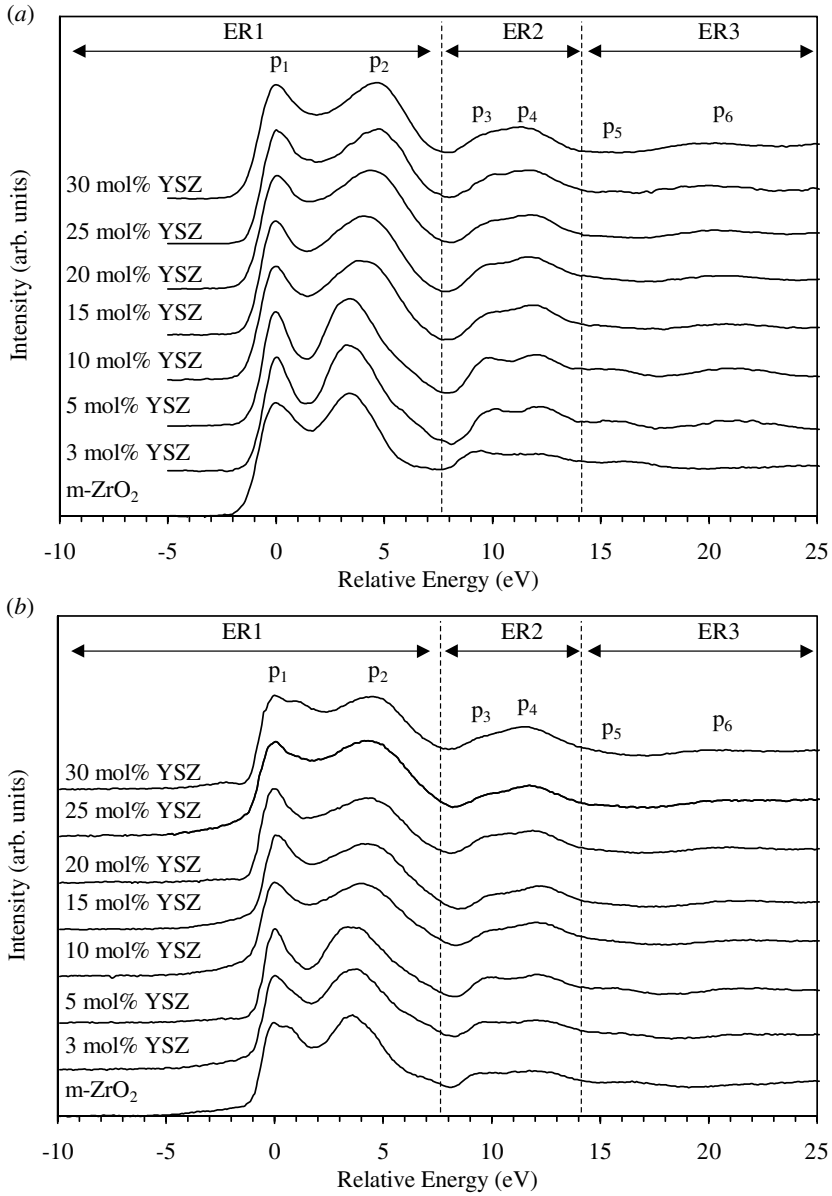


**Figure 2.** Oxygen K-edge ELNES (*a*) and XANES (*b*), for the specimens investigated. The XANES data shown have been corrected for the effects of specimen charging.

In ER3 a rather weak feature, $p_5$, can be observed in the monoclinic and tetragonal phases but this feature is absent in the cubic materials. This peak appears to occur at lower energy-loss in the tetragonal phases than in the monoclinic phase. In addition there is a very broad peak, $p_6$, at relative energy-loss of ∼22 eV, which is present in all the phases.

Figure 2(*b*) shows the oxygen K-edge XANES data from the range of zirconia samples investigated. All of the data shown in figure 2(*b*) have been corrected for the effects of specimen charging. The lack of spatial resolution in the XANES experiments means that the spectra

recorded are due to excitations in a large number of grains in the specimen. This is particularly significant in the case of the 20 and 25 mol% YSZ samples, where the EDX analyses revealed that the yttria distributions are inhomogeneous. Similarly it should be noted that the XRD measurements of the tetragonal samples revealed the presence of other zirconia phases, albeit at a low concentration. It is worth emphasizing that specimen inhomogeneity or the presence of minority phases will potentially complicate the analysis of XANES data while, in contrast, since the ELNES experiments were performed on individual grains of known yttrium metal fraction the interpretation is more straightforward.

Nevertheless, an initial analysis of figure 2(*b*) reveals that the trends observed in the ELNES data are all reproduced in the XANES spectra. In particular the dependence of the energy difference between $p_1$ and $p_2$ noted in the ELNES data is also apparent in the XANES data as are the changes in the shape and number of the peaks in ER2. One additional feature that can be identified in the XANES data is the splitting of the first peak, $p_1$, in the spectra of m-$ZrO_2$ and 30 mol% YSZ. This feature is not present in the ELNES data from either of these specimens and is likely to be associated with sudden discharging of the insulating ceramic grains during data collection. This effect cannot be corrected using the charge correction algorithm described in [19].

The detailed theoretical interpretation of the near-edge structure on the oxygen K-edge has been discussed elsewhere [5, 7]. In the initial study by McComb [20] the two major peaks, $p_1$ and $p_2$, were interpreted as being due to excitations into unoccupied p-like states on the oxygen site formed by overlap between the oxygen 2p wavefunctions and zirconium 4d wavefunctions. However, these d orbitals will not be degenerate due to the point symmetry at the metal sites. In the simplest case of pure cubic $ZrO_2$ this can be viewed as a ligand field splitting into a lower energy doubly degenerate level ($e_g$) and a triply degenerate level ($t_{2g}$) that will be higher in energy. Thus, the p-projected local DOS at the oxygen sites will reflect this splitting through the interaction of the oxygen 2p and zirconium 4d wavefunctions. However this simplistic view provides only limited insight. In fact the local environment around the zirconium ion in m-$ZrO_2$, the only pure phase that is stable at ambient temperature, is seven coordinate with three long and four short Zr–O bonds. In the tetragonal and cubic phases, the environments are even more complex since aliovalent dopant ions and oxygen vacancies are also present. Previously published results have shown that this complexity must be taken into account in calculations of the electronic structure and ELNES/XANES of YSZ materials [5, 7].

From the ELNES and XANES data presented in figure 2, it can be concluded that analysis of near-edge structure provides a rapid method for identification of the crystallographic phase of YSZ confirming the earlier work by McComb [20]. The monoclinic phase can be easily distinguished from other phases by the shallow minimum between ER1 and ER2 as well as by the shape of the features in ER2. More significant is the ability to distinguish between the tetragonal and cubic phases. The tetragonal distortion is relatively weak ($c/a \approx 1.015$), which means that in a randomly oriented powder or ceramic material it can be problematic to distinguish between such phases using electron diffraction in the TEM [9]. For this reason the morphology of the grains is often used as a method of identification. However, the grain morphology may be dependent on the method of preparation and therefore a rapid technique that provides reliable identification of phase is extremely powerful [21]. The cubic and tetragonal phases are easily distinguished using ELNES and XANES by the depth of the minimum between $p_1$ and $p_2$ in ER1 and by the splitting of the features observed in ER2. The energy separation between $p_1$ and $p_2$ is related to the crystallographic phase but as will be become clear in the following discussion this is a less reliable method of phase identification.

In both the ELNES and the XANES results, it is clear that the energy difference between $p_1$ and $p_2$ in the oxygen K-edge data increases as the $Y_2O_3$ concentration increases. This energy difference, $\Delta E_{p2-p1}$, has been measured in all of the materials investigated and is plotted in

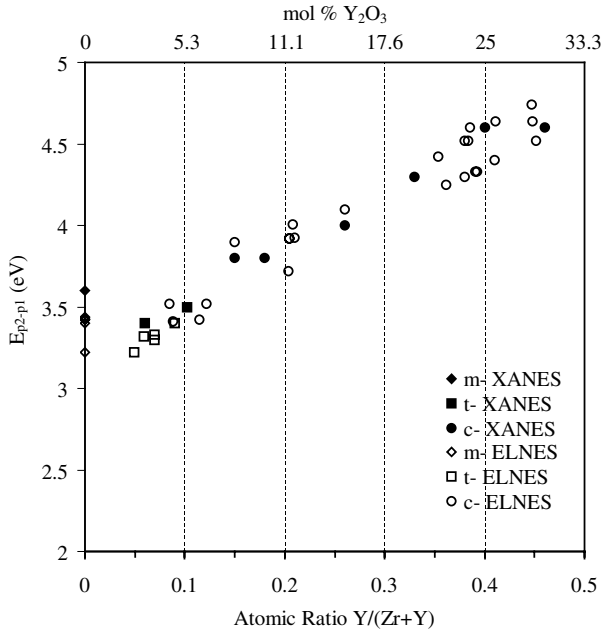


**Figure 3.** Plot of the energy difference between the first two peaks ($\Delta E_{p2-p1}$) in the oxygen K-edge as a function of the ratio of Y/(Y + Zr) in the specimens investigated. The legend indicates the measurement technique used as well as the crystallographic phase of the sample. In the XANES data this is the phase determined by XRD measurements while in the ELNES cases the phase was assigned to each grain on the basis of the observed fine structure in the recorded ELNES data.

figure 3 against the metal fraction of yttrium. The legend shows both the technique used and the crystallographic phase assigned to the data point. In the case of the XANES data, the yttrium metal fraction corresponds to the nominal value for the sample used and the phase is the dominant phase determined from the XRD pattern. For each ELNES data point, the metal fraction of yttrium was measured by EDX analysis on the same sample grain and the phase was determined from the ELNES shape.

In figure 3 it can be seen that the values of $\Delta E_{p2-p1}$ measured from ELNES and XANES data follow the same trend and appear to be linearly dependent on the metal fraction of yttrium for the tetragonal and cubic phases. The data points for the monoclinic phase lie a little above this trend line. It should be noted that the value of the splitting obtained from XANES of m-$ZrO_2$ and 30 mol% YSZ are likely to be unreliable due to the extra feature, attributed to specimen discharging, that is present on $p_1$. If there are grains with a range of metal fractions in the irradiated volume, as in the case of the XANES recorded from the 20 and 25 mol% YSZ samples, this will be reflected in the broadening of $p_2$, providing a method of detecting such inhomogeneity in a bulk sample.

Clearly it can be concluded from the data presented that $\Delta E_{p2-p1}$ is a sensitive measure of the yttrium metal fraction present in YSZ materials. This ability in combination with the ability to identify the crystallographic phase of each grain makes spatially resolved ELNES an extremely powerful analytical technique for the investigation of inhomogeneities in YSZ.

## 4. Conclusions

This work has demonstrated that near-edge structure at the oxygen K edge is a powerful technique for investigation of YSZ materials providing information on both phase and composition. It has been shown that, although the same features are present on the oxygen K edge measured by both XANES and ELNES, there are significant discrepancies in the peak intensities in the raw data. This is due to the effect of specimen charging during XANES analysis. The effect of specimen charging can be measured directly and the data can be processed to reduce the discrepancies between the techniques.

Investigation of a series of YSZ samples with systematically varying compositions has revealed that near-edge structure analysis can be used to reliably identify the crystallographic phase of the material. In addition, it has been demonstrated for the first time that the energy difference between the first two peaks of the oxygen K edge is directly related to metal fraction of yttrium present in the analysed region.

The results of this study are extremely significant due the spatial resolution of the ELNES technique when carried out in a modern analytical electron microscope. In current commercial instruments this type of analysis can be performed with a spatial resolution of 0.2 nm with an acquisition time of about 4 s. Thus, using ELNES, it is possible to probe simultaneously the structure and chemistry at homogeneous and heterogeneous interfaces in technical ceramics, sensors and fuel cells based on stabilized zirconia materials.

## Acknowledgments

The authors would like to thank Ian Kirkman (Daresbury), Jim Gallagher, Sam McFadzean, Murdo McLeod and Bill Higginson for their help in this work. We are grateful to EPSRC (GR/L66953), MEL Chemicals and Johnson Matthey for their support in carrying out this work.

## References

[1] Subbarao E C 1981 *Science and Technology of Zirconia Advances in Ceramics* vol 3, ed A H Heuer and L W Hobbs (Columbus, OH: American Ceramic Society)
[2] Stevens R 1986 *Zirconia and Zirconia Ceramics (Magnesium Electron Publication No. 113)* (Manchester: Magnesium Electron)
[3] Howard C J, Hill R J and Reichert B E 1988 *Acta Crystallogr.* B **44** 116
[4] Ohtaka O, Yamanaka T, Kume S, Ito E and Navrotsky A 1991 *J. Am. Chem. Soc.* **74** 505
Ohtaka O, Yamanaka T and Yagi T 1994 *Phys. Rev.* B **49** 9295
[5] Ostanin S, McComb D W, Craven A J, Vlachos D, Alavi A, Finnis M W and Paxton A T 2001 *Phys. Rev.* B submitted
[6] Fabris S, Paxton A T and Finnis M W 2001 *Phys. Rev.* B **63** 094101
[7] Ostanin S, McComb D W, Craven A J, Vlachos D, Alavi A, Finnis M W and Paxton A T 2000 *Phys. Rev.* B **62** 14 728
[8] Goff J P, Hayes W, Hull S, Hitchings M T and Clausen K N 1999 *Phys. Rev.* B **59** 14 202
[9] Kondoh J, Kikuchi S, Tomii Y and Ito Y 1999 *Physica* B **262** 177
[10] Tuilier M H, Dexpert-Ghys J, Dexpert H and Lagarde P 1987 *J. Solid State Chem.* **69** 153
[11] Li P, Chen W and Penner-Hahn J E 1993 *Phys. Rev.* B **48** 10 063
Li P, Chen W and Penner-Hahn J E 1993 *Phys. Rev.* **48** 10 082
[12] Egerton R F 1996 *Electron Energy-Loss Spectroscopy in the Electron Microscope* 2nd edn (New York: Plenum)
[13] De Groot F M F 1994 *J. Electron Spectrosc. Relat. Phenom.* **67** 529
[14] Sawatzky G A 1991 *Microsc. Microanal. Microstruct.* **2** 153

[15] Muller J E and Wilkins J W 1984 *Phys. Rev.* B **29** 4331
Muller D A, Singh J and Silcox J 1998 *Phys. Rev.* B **57** 8181
Nelhiebel M, Louf P H, Schattschneider P, Blaha P, Schwarz K and Jouffrey B 1999 *Phys. Rev.* B **59** 12 807
Ankudinov A L, Ravel B, Rehr J J and Conradson S D 1998 *Phys. Rev.* B **58** 7565
Bogicevic A, Wolverton C, Crosbie G M and Stechel E B 2001 *Phys. Rev.* B **64** 014106
[16] Hjalmanson H P, Buttner H and Dow J D 1981 *Phys. Rev.* B **24** 6010
[17] Lie K, Hoier R and Brydson R 2000 *Phys. Rev.* B **61** 1786
[18] Paxton A T, van Schilfgaarde M, MacKenzie M and Craven A J 2000 *J. Phys.: Condens. Matter* **12** 729
[19] Vlachos D, McComb D W and Craven A J 2001 *J. Synchrotron Radiat.* submitted
[20] McComb D W 1996 *Phys. Rev.* B **54** 7094
[21] Ross I M, Rainforth W M, McComb D W, Scott A J and Brydson R 2001 *Scr. Mater.* **45** 653